Research Article | Vol. 6, No. 11 | 1 Nov 2016 | OPTICAL MATERIALS EXPRESS 3586

Optical Materials EXPRESS

Annealing-induced phase transition in zinc phthalocyanine ultrathin films

HYEYOUNG AHN* AND TING-CHANG CHU

Department of Photonics, National Chiao Tung University, Hsinchu 30010, Taiwan
**hyahn@mail.nctu.edu.tw*

Abstract: We report the evidence of post-annealing-induced phase transition in zinc phthalocyanine (ZnPc) ultrathin (~20 nm) films upon annealing at 200 °C. The signatures of phase transition are observed in their morphological, structural, and ultrafast spectroscopic properties. X-ray diffraction measurement shows that α-phase nanospheres transform to β-phase nanorods that have a high degree of crystallinity with an excellent ordering along the *c*-direction in a monoclinic arrangement. Tight packing of molecules in the β-crystallites allows a red-shift and intensity gain of the lowest-energy subband in the Q-band and subsequently increases the electronic coupling in both intercolumn and intracolumn paths.

OCIS codes: (320.7150) Ultrafast spectroscopy; (160.4236) Nanomaterials.

References and links

1. V. S. Williams, S. Mazumda, N. R. Armstrong, Z. Z. Ho, and N. Peygharmbarian, "Femtosecond excited-state dynamics in fluoro- and chloroaluminum phthalocyanine thin films," J. Phys. Chem. **96**, 4500 (1992).
2. A. Terasaki, M. Hosoda, T. Wada, H. Tada, A. Koma, A. Yamada, H. Sasabe, A. F. Garito, and T. Kobayashi, "Femtosecond spectroscopy of vanadyi phthalocyanines in various molecular arrangements," J. Phys. Chem. **96**(25), 10534–10542 (1992).
3. V. Gulbinas, M. Chachisvilis, L. Valkunas, and V. Sundstrom, "Excited state dynamics of phthalocyanine films," J. Phys. Chem. **100**(6), 2213–2219 (1996).
4. L. Howe and J. Z. Zhang, "Ultrafast studies of excited-state dynamics of phthalocyanine and zinc phthalocyanine tetrasulfonate in solution," J. Phys. Chem. A **101**(18), 3207–3213 (1997).
5. J. Zhou, J. Mi, R. Zhu, B. Li, and S. Qian, "Ultrafast excitation relaxation in titanylphthalocyanine thin film," Opt. Mater. **27**(3), 377–382 (2004).
6. S. Kakade, R. Ghosh, and D. K. Palit, "Excited state dynamics of Zinc–phthalocyanine nanoaggregates in strong hydrogen bonding solvents," J. Phys. Chem. C **116**(28), 15155–15166 (2012).
7. M. Szybowicz, T. Runka, M. Drozdowski, W. Bała, M. Wojdyła, A. Grodzicki, P. Piszczek, and A. Bratkowski, "Temperature study of Raman, FT-IR and photoluminescence spectra of ZnPc thin layers on Si substrate," J. Mol. Struct. **830**(1-3), 14–20 (2007).
8. H. Ahn, W.-H. Liou, H.-M. Chen, and C.-H. Hsu, "Anisotropic exciton relaxation in nanostructured metal (Zn and $F_{(16)}$Zn)-phthalocyanine," Opt. Express **23**(3), 3230–3235 (2015).
9. A. Chowdhury, B. Biswas, M. Majumder, M. K. Sanyal, and B. Mallik, "Studies on phase transformation and molecular orientation in nanostructured zinc phthalocyanine thin films annealed at different temperatures," Thin Solid Films **520**(21), 6695–6704 (2012).
10. D. Roy, N. M. Das, N. Shakti, and P. S. Gupta, "Comparative study of optical, structural and electrical properties of zinc phthalocyanine Langmuir–Blodgett thin film on annealing," RSC Advances **4**(80), 42514–42522 (2014).
11. X. He, G. Zhu, J. Yang, H. Chang, Q. Meng, H. Zhao, X. Zhou, S. Yue, Z. Wang, J. Shi, L. Gu, D. Yan, and Y. Weng, "Photogenerated Intrinsic Free Carriers in Small-molecule Organic Semiconductors Visualized by Ultrafast Spectroscopy," Sci. Rep. **5**, 17076 (2015).
12. S. Heutz, S. M. Bayliss, R. L. Middleton, G. Rumbles, and T. S. Jones, "Polymorphism in phthalocyanine thin films: Mechanism of the α→β transition," J. Phys. Chem. B **104**(30), 7124–7129 (2000).
13. H. Laurs and G. Heiland, "Electrical and optical properties of phthalocyanine films," Thin Solid Films **149**(2), 129–142 (1987).
14. A. Stradomska and J. Knoester, "Shape of the Q band in the absorption spectra of porphyrin nanotubes: Vibronic coupling or exciton effects?" J. Chem. Phys. **133**(9), 094701 (2010).
15. N. Kobayashi, T. Fukuda, and D. Lelievre, "Band Deconvolution Analysis of the Absorption and Magnetic Circular Dichroism Spectral Data of ZnPc(-2) Recorded at Cryogenic Temperatures," J. Phys. Chem. **99**, 7935–7945 (1995).
16. JCPDS-ICDD stands for the joint committee on powder diffraction standards-the international center for diffraction data.
17. M. K. Debe, "Variable angle spectroscopic ellipsometry studies of oriented phthalocyanine films. II. copper phthalocyanine," J. Vac. Sci. Technol. A **10**(4), 2816–2821 (1992).

#268972 http://dx.doi.org/10.1364/OME.6.003586
Journal © 2016 Received 23 Jun 2016; revised 30 Sep 2016; accepted 21 Oct 2016; published 26 Oct 2016

Optical Materials EXPRESS

18. F. H. Moser and A. L. Thomas, Phthalocyanine Compounds, ACS Monograph Series 157, American Chemical Society: New York (1963).
19. R. O. Loutfy, "Bulk optical properties of phthalocyanine pigment particles," Can. J. Chem. **59**(3), 549–554 (1981).
20. G. Guillaud, J. Simon, and J. P. Germain, "Metallophthalocyanines gas sensors, resistors and field effect transistors," Coord. Chem. Rev. **178–180**, 1433–1484 (1998).
21. S. Yim, H. Heutz, and T. S. Jones, "Model for the $\alpha \rightarrow \beta_1$ phase transition in phthalocyanine thin films," J. Appl. Phys. **91**(6), 3632–3636 (2002).
22. L. D. A. Siebbeles, A. Huijser, and T. J. Savenije, "Effects of molecular organization on exciton diffusion in thin films of bioinspired light-harvesting molecules," J. Mater. Chem. **19**(34), 6067–6072 (2009).
23. S. V. Rao and D. N. Rao, "Excited state dynamics in phthalocyanines studied using degenerate four wave mixing with incoherent light," J. Porphyr. Phthalocyanines **6**(03), 233–237 (2002).
24. H. Abramczyk, B. Brozek-Pluska, M. Tondusson, and E. Freysz, "Ultrafast dynamics of metal complexes of tetrasulfonated phthalocyanines at biological interfaces: Comparison between photochemistry in solutions, films, and noncancerous and cancerous human breast tissues," J. Phys. Chem. C **117**(10), 4999–5013 (2013).
25. G. Giri, E. Verploegen, S. C. B. Mannsfeld, S. Atahan-Evrenk, D. H. Kim, S. Y. Lee, H. A. Becerril, A. Aspuru-Guzik, M. F. Toney, and Z. Bao, "Tuning charge transport in solution-sheared organic semiconductors using lattice strain," Nature **480**(7378), 504–508 (2011).

1. Introduction

Phthalocyanines (Pcs) are two-dimensional aromatic molecules with an inner ring. The π-π orbital overlap and electrostatic interactions between adjacent Pc cores induce disc-like Pc molecules to self-assemble into one-dimensional columnar structures in condensed phases. Metallophthalocyanine (MPc) has a central metal atom and its optical and chemical properties depend on the variation of the metal atom and the position and nature of substitute atoms. Therefore, the knowledge of the precise morphology, the microscopic molecular arrangement, and excited-state dynamics are essential for their prospective applications [1–6]. Zinc phthalocyanines (ZnPc) present of particular interest due to their high absorption coefficient and high energy conversion efficiency in UV-VIS range. As-fabricated ZnPc has a planar coordination around the central ion and shows D_{4h} planar symmetry at room temperature [7]. Thin layers of ZnPc can be spin coated or evaporated from solution on nearly any solid state substrate and the easy synthesis makes them particularly attractive for future practical applications of cheap and highly stable large-area molecular electronic devices.

The ZnPc films deposited at room temperature are often grown in the form of nanostructures, such as nanospheres or vertically-aligned nanorods [8]. Thermal annealing of ZnPc films can induce the phase transition from the α to β polymorph and morphologically transform spherical grains into elongated nanorods aligned parallel to the substrate [9,10]. For ZnPcs, the ultrafast excitonic dynamics has been well characterized until recently a band-like electronic transition was proposed for highly crystalline ZnPc films with long-range ordering [11]. Meanwhile, due to kinetical constraint, annealing-induced phase transition in the ZnPc thin films of thickness lesser than 100 nm is rarely observed [12], but the influence of thickness on the phase transition is still of fundamental interest. In this work, we prepared the ZnPc ultrathin films with nominal thickness of 20 and 50 nm and observed a clear evidence of phase transition when they are annealed at temperatures greater than 200 °C. It is known that the visible absorption band (Q-band) of ZnPc is composed of four subbands. Although there have been several reports on the redshift and the relative change of intensity of subbands depending on the geometry and the crystalline structures [13,14], the transient behavior of these subbands associated with the dynamics of excited state is still not well known. Therefore, in this work we redefine the role of the lowest-energy subband in the excited state dynamics during the phase transition and its relation with the structural transformation. In the study of X-ray diffraction (XRD) and ultrafast spectroscopy, long β-phase nanorods are found to have a very high crystallinity and its long-range character was acquired through the increase of tilt angle and the deformation of planar disk, which distinctively enhance intra- and intercolumnar interactions.

Optical Materials EXPRESS

2. Experimental methods

ZnPc thin films were deposited on pre-cleaned glass substrates at room temperature using a thermal evaporation technique. ZnPc thin films with thicknesses of ~20 nm and 50 nm were fabricated under a vacuum pressure less than 5×10^{-6} Torr. The deposition rate was kept at 0.1-0.2 Å/sec and the thickness of film was controlled by measuring the shifts in resonance frequency of a quartz crystal detector. After deposition, the ZnPc films were annealed at different temperatures (T) ranging from 100 to 250 °C under a vacuum pressure of ~1×10^{-4} Torr for 15 minutes. Annealing for longer time causes the reduction of optical absorption, which may be attributed to the sublimation of the film.

The molecular orientation and the crystalline quality were determined through grazing-incident x-ray diffraction (GIXRD) taken with the x-ray wavelength of 1.03321 Å at an incident angle of 0.1 or 0.2° at beamline BL01C2 of the National Synchrotron Radiation Research Center, Taiwan. The morphology and thickness of each film were analyzed using field emission scanning electron microscopy (FESEM). The absorption spectra of samples were measured by an UV-VIS-NIR spectrophotometer in the wavelength range of 300 – 1200 nm. Ultrafast pump-probe measurements were performed using a Ti:sapphire laser system, which delivers ~150 fs optical pulses at central wavelengths tunable from 700 to 1000 nm. Orthogonally polarized single color pump and probe pulses were noncollinearly overlapped with the angle difference of 45°. The fluence of the pump beam was typically 30 MW/cm^2 and all the measurements were performed at room temperature. Our Pc samples have two major absorption bands; B-band in the UV spectra and Q-band in the VIS/NIR region. In order to elucidate the absorption kinetics near the absorption edge, laser pulses in the wavelength range of 700 – 800 nm were used to create and probe photocarriers in the Q-band of ZnPc.

3. Results and discussion

Figures 1(a)–1(c) depict the SEM images of 20 nm-thick ZnPc films, as-deposited, annealed at 150 °C [ZnPc-(150)], and 200 °C [ZnPc-(200)], respectively. As-deposited film is composed of nearly spherical granular crystallites with an average size of 20 nm. The top-view image of ZnPc-(150) in Fig. 1(b) shows that a few elongated rod-like nanostructures appears on the top of nanospheres, whose long axis is parallel to the substrate. These nanorods do not appear in the as-deposited and ZnPc-(100) films [not shown]. After annealed at 200 °C, small ZnPc nanospheres completely transform to very long horizontally-lying nanorods, as it is shown in Fig. 1(c). The formation of nanorods is known to be the result of free energy minimization because Pc molecules prefer plane-on-plane arrangement of molecules to plane-by-plane arrangement [9,10]. Previously, it was suggested that this structural transformation may occur only for films thicker than ~100 nm [12], but the image in Fig. 1(c) demonstrates that the structural phase transition to nanorods can occur in the 20 nm-thick films. A similar morphological transition was observed in a thicker (50 nm) film annealed at 200 °C.

The absorption spectra of as-deposited and annealed films are shown in Fig. 1(d)–1(f). Like other Pcs, ZnPc molecules strongly absorb the red region of solar spectrum (Q-band). The absorption curve of ZnPc-(100) [not shown] is essentially the same as that of the as-deposited film. It is known that the two broad peaks in the Q-band come from $n \rightarrow \pi^*$ and $\pi \rightarrow \pi^*$ transitions in combination with the Davydov doublet splitting bands [11,12]. And multi-component fitting of the absorption spectra shows that there are four distinct vibrational subbands (Q_1 – Q_4) in the Q-band and they are shown as grey lines under the sum spectra [13–15]. With the increase of annealing temperature to 150 °C, bands Q_3 and Q_4 shift to longer wavelengths, while bands Q_1 and Q_2 to shorter wavelengths. After annealing at 200 °C, the intensity of the band Q_4 is significantly increased. These characteristic changes in the absorption curves are related with the polymorphic phase transition from α to β .

Optical Materials EXPRESS

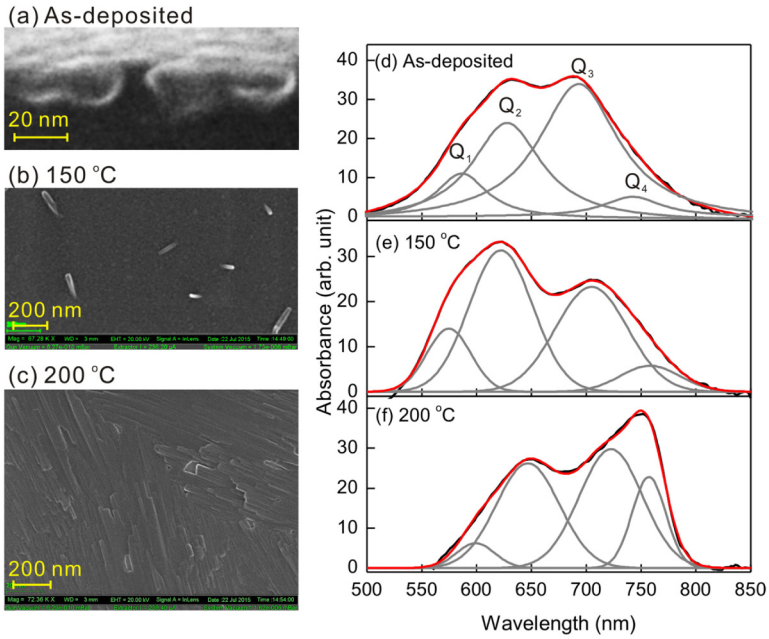

Fig. 1. FESEM images (a)-(c) and absorption spectra (d)-(f) of 20 nm-thick ZnPc films, as-deposited and annealed at 150 and 200 °C. The 50-nm thick film shows similar morphology and absorption responses. Red solid lines in Fig. 1(d)-(f) are results of multipeak fitting.

The annealing-induced phase transition is also observed in GIXRD measurement. Figures 2(a) and 2(b) show the out-of-plane and in-plane XRD curves, respectively. The out-of-plane XRD pattern of the as-deposited film exhibits the polycrystalline nature, as evidenced by a single major diffraction peak q_1 $\left(=\frac{4\pi}{\lambda}\sin\theta\right)$ at ~0.487 Å^{-1} accompanied by a broad amorphous hump near 1.68 Å^{-1}. The major peak corresponding to *d*-spacing = 12.89 Å for the as-deposited film is due to diffraction from (100) (triclinic phase) or (200) (monoclinic phase) planes with ordered arrangement of edge-on ZnPc molecules [16]. Inset in Fig. 2(a) exhibits the annealing temperature dependence of the peak position and the full width at half maximum (FWHM). The shift of q_1 from 0.487 Å^{-1} to 0.502 Å^{-1} corresponds to the decrease of *d*-spacing from 12.89 Å to 12.52 Å, implying that the Pc rings tend to incline to the substrate surface. The increase of peak intensity and the decrease of FWHM for ZnPc-(200) confirm the higher crystallinity in β-ZnPc films. The inset in Fig. 2(a) shows a slight shift of peak position as well as FWHM of XRD curve for ZnPc-(150), indicating that there is an ongoing partial phase transition in ZnPc-(150).

The in-plane XRD curve in Fig. 2(b) exhibits more significant temperature-dependent features. The XRD curves of as-deposited and ZnPc-(100) films are nearly the same. This indicates that there is no structural change during low temperature annealing. As the annealing temperature increases to 150 °C, the primary peak at ~0.51 Å^{-1} (*d* = 12.32 Å) becomes more intense and narrower, indicating that the ZnPc-(150) film has higher crystalline order. After annealing at 200 °C, the primary peak at 0.51 Å^{-1} completely disappears and concomitantly, several new diffraction peaks appear in the ZnPc-(200) film [also see the inset in Fig. 2(b)]. Multiple peaks in new positions imply that there is a significant structural transformation during the phase transition in terms of plane orientation and interplanar spacing along the in-plane direction. The peak intensity of the in-plane response is relatively

Optical Materials EXPRESS

small, but it can be clearly identified in the XRD pattern in Fig. 2(c) and the same in-plane X-ray signatures were also observed in 50-nm films annealed at 200 °C.

It is well known that the β-ZnPc crystallites have monoclinic unit cell with a tilt angle (β = 106.15°) between the *a*- and *c*-axis, whereas the α-ZnPc belongs to tetragonal or orthorhombic symmetry [17–19]. In the β-ZnPc, the *b*-axis of molecular columns is parallel to the long axis of nanorods as well as the substrate. There are a limited number of stacking ways for monoclinic unit cells, such as inversion (A) and rotation (B) around *b*-axis, as it is shown in Fig. 2(d). The diffraction peaks in XRD curves corresponds to different stacking modes with different periodicity. In Fig. 2(a), there is only a single main peak in the out-of-plane XRD curves for both as-deposited and annealed films. This result indicates that the vertically tilted stacking of cells like the B-mode in Fig. 2(d) may be unlikely to occur in the 20-nm ZnPc film [20,21]. Then the multi peaks in the in-plane XRD signals of ZnPc-(200) correspond to the appearance of new periodicity associated with the planar orientation (like A-mode) and translation of tilted cuboids.

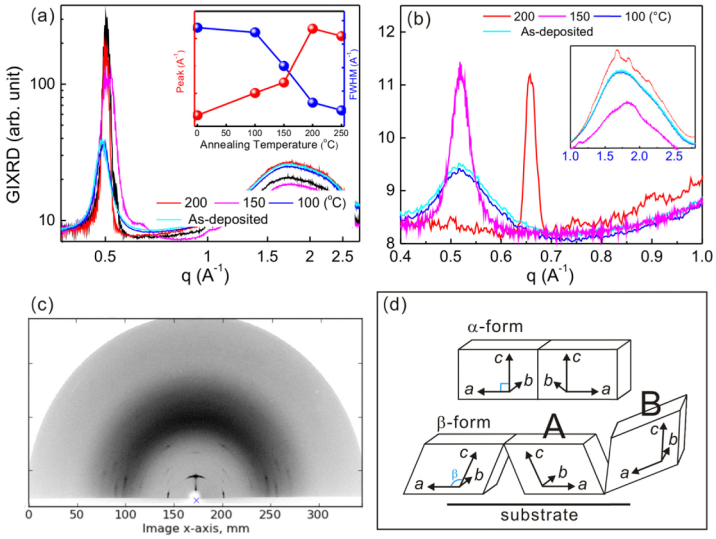

Fig. 2. X-ray diffraction curves of ZnPc films as-deposited and annealed at different temperatures in the directions normal- (a) and parallel (b) to the substrate plane, respectively. Inset in (a) is the temperature dependence of the position and FWHM of out-of-plane peak and the one in (b) is the XRD curve at larger q. (c) Half-circle XRD pattern for ZnPc-(200). (d) Schematics of unit cells packing in α-form and β-form ZnPcs.

The influence of annealing on the excited state dynamics is investigated using the pump-probe technique. Figure 3(a) exhibits the annealing temperature dependence of transient transmittance (DT = ΔT/T) for the *s*-polarized probe beam at a wavelength of 740 nm. With photoexcitation, all DT signals sharply increase followed by an initially rapid decline and subsequently gradual decrease. The exponential decay profiles of DTs are analyzed by two characteristic time constants (τ_1 and τ_2). An additional long-lifetime component (τ_3) retains more than the limit of our temporal scanning range so that we set it to be 1000 ps for fitting of each curve. The inset in Fig. 3(a) shows the wavelength dependence of τ_1 and τ_2 for three samples: as-deposited, annealed at 150 and 200 °C. The singlet lifetime τ_2 of about 60 ps [22,23] decreases significantly to about 30 ps after phase transition. Interestingly, an additional ultrafast decay with a time constant (τ_0) of 1-1.5 ps (solid pink squares) was observed in the ZnPc-(150) film at wavelengths greater than 740 nm. This may correspond to the fast decay of small population of carriers excited to the band Q_4 in the intermediate status of ZnPc-(150), as it will be discussed below. Figure 3(b) exhibits the DT of ZnPc-(200) measured at different probe wavelengths. The positive rise of DT flips its sign to negative at

Optical Materials EXPRESS

~720 nm. The positive step-like rise of DT is due to the instantaneous photobleaching and the flip of sign indicates the increased contribution of excited state absorption that is dominant at the central region of Q-band absorption spectrum [1–6]. Similar temperature and wavelength dependences of carrier dynamics were observed for 50 nm-thick film.

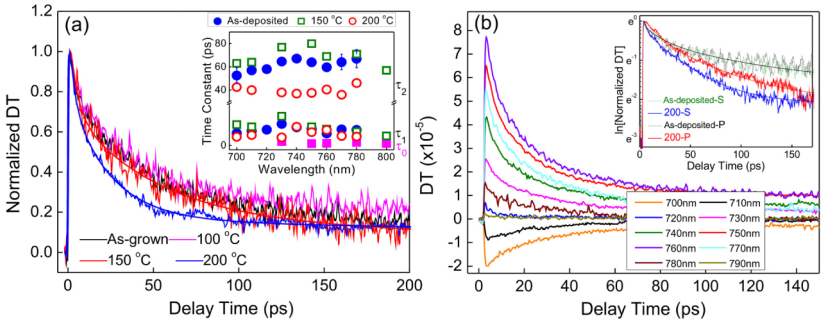

Fig. 3. (a) Annealing temperature dependence of the normalized DT at 740 nm. Inset: time constant vs. wavelength for the films as-deposited (solid circles), and annealed at 150 °C (open squares) and 200 °C (open circles). Pink solid squares correspond to τ_0 of ZnPc-(150). (b) Probe wavelength dependence of the ZnPc-(200) film. Inset: Polarization dependence of normalized DT for films as-deposited and annealed at 200 °C.

Figures 4(a)–4(c) show the transmittance spectra at discrete time intervals for the samples as-deposited, and annealed at 150 and 200 °C, respectively. Solid grey curves in each figure correspond to the two absorption subbands (Q_3 and Q_4) in adjusted magnitudes. For the as-deposited sample, the DT at 0.2 ps quantitatively agrees with the band Q_3. This indicates that most photogenerated carriers are excited to the band Q_3 centered at ~690 nm for α-ZnPc. Similar bleaching was observed for ZnPc-(200), but in this case, the photocarriers are excited to the band Q_4. For the ZnPc-(150) film in Fig. 4(b), the initial absorption occurs both in bands Q_3 and Q_4, and the carriers in the band Q_4 decay rapidly within 3 ps. The results of ZnPc-(150) describe the intermediate state consisting of coexisting α and β phases.

Previously, the appearance of an additional band near the absorption edge has been observed in the weak-epitaxy-grown ZnPc films having rodlike structure by He *et al.* [11]. According to them, the additional band is related to the long-range periodicity of the crystal lattice and its excited state dynamics shows the band-like electronic behavior following the second-order rate of electron-hole recombination. Figures 4(d)–4(f) show the reciprocal of kinetics traces (1/DT) at 700 nm. The response at 770 nm was also shown for comparison in Fig. 4(f). The strong linearity refers to their good agreement with a bimolecular recombination mechanism. As the annealing temperature increases, the recombination rate constant (k_e) obtained from the slope of linear trace at 700 nm increases from 0.020 ps^{-1} to 0.044 ps^{-1} and it is the same as the value at 770 nm. The significant increase of k_e with phase transition indicates the enhancement of electronic coupling resulted from the decrease of *d*-spacing. Since each subband in the Q-band corresponds to different vibrational mode, the increase of k_e with the shift of prominent subband from Q_3 to Q_4 indicates that there may be a change in molecular symmetry, probably from D_{4h} to C_{4v} [24,25], during the phase transition process. Similar enhancement of k_e has been observed for the derivatives of Pc and porphyrin when the molecular planes are largely tilted toward the stack direction [22].

Optical Materials EXPRESS

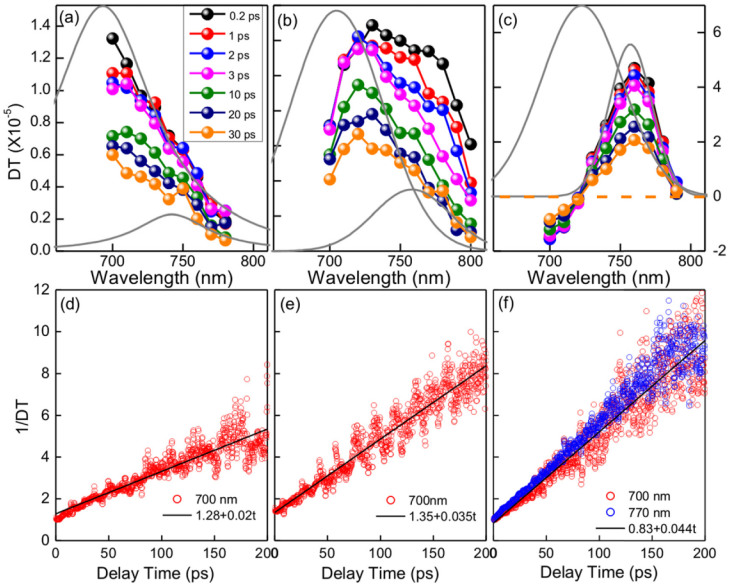

Fig. 4. DT spectra at discrete time intervals (a)–(c) and 1/DT measured at 700 nm (d)–(f) for the films as-deposited, and annealed at 150 and 200 °C, respectively. Solid lines are linear fit to 1/DT at 700 nm.

The inset in Fig. 3(b) exhibits the polarization dependence of DT at 740 nm measured for as-deposited and ZnPc-(200) films. The decay of DT for the as-deposited film does not depend on the polarization of probe beam, while that of DT for ZnPc-(200) exhibits strong polarization dependence. In particular, the *p*-polarized DT which specifies the out-of-plane interaction decays mono-exponentially with a 31 ps lifetime. We learned from above that the decrease in τ_2 (increase in k_e) is due to the reduction of intercolumn distance. Thus, the fast mono-exponential decay of *p*-polarized DT for ZnPc-(200) indicates that the phase transition permits tighter and highly ordered parallel stacking of columns along the out-of-plane direction in nanorods. The bi-exponential response of *s*-polarized DT reflects the electronic coupling associated with the intracolumn as well as intercolumn path. The fast time constant τ_1 of the order of several ps corresponds to the intracolumnar coupling due to vibrational relaxation in the first excited singlet [22,23]. The slight decrease of τ_1 after phase transition may be related to the decrease of π–π distance due to changes in molecular symmetry of ZnPc. At high temperature, it is known that the Zn atom adopts a position out of the plane of the ring and a significant doming changes the symmetry of molecule [24].

4. Summary

We have demonstrated the influence of the α→β phase transition on the crystalline structure and the relaxation dynamics of excited state in the ZnPc ultrathin films. Upon annealing above 200 °C, small nanospheres with diameter of about 20 nm transform to elongated nanorods (longer than 1 μm) laid parallel to the substrate surface. The out-of-plane XRD analysis shows that the tilt angle of planar molecules within the columns increases with increasing annealing temperature. This leads to a relatively short intercolumn distance and allows significant interaction in adjacent columns. The in-plane ordering of molecules in nanorods is achieved by tight and parallel arrangement of monoclinic cells along the substrate surface. We found that high crystallinity of the β-ZnPc film leads two low-energy subbands in the Q-band (Q_3 and Q_4) to exchange the role in determination of the excited state dynamics during the phase transition process. The electronic coupling in the band Q_4 is markedly

Optical Materials EXPRESS

stronger than that in the band Q_3 and improves the carrier transport properties in the β-ZnPc nanorods.

Funding

Ministry of Science and Technology (MOST-104-2112-M-009-007-MY3); the Science Vanguard Research Program (MOST-104-2628-M-007-001).